Arch Virol (2010) 155:1107–1116
DOI 10.1007/s00705-010-0693-1

ORIGINAL ARTICLE

Classical swine fever virus down-regulates endothelial connexin 43 gap junctions

Hsiang-Jung Hsiao · Pei-An Liu · Hung-I Yeh · Chi-Young Wang

Received: 16 July 2009 / Accepted: 26 February 2010 / Published online: 16 May 2010

Abstract Classical swine fever is a contagious disease of pigs characterized by fatal hemorrhagic fever. Classical swine fever virus (CSFV) induces the expression of pro-inflammatory and pro-coagulant factors of vascular endothelial cells and establishes a long-term infection. This study aimed to understand the effect of CSFV on endothelial connexin 43 (Cx43) expression and gap junctional intercellular coupling (GJIC). Porcine aortic endothelial cells were infected with CSFV at different multiplicity of infection for 48 h. Semi-quantitative RT-PCR, immunoconfocal microscopy, and Western blotting showed that the transcription and translation of Cx43 were reduced, and this was associated with an attenuation of GJIC. This decrease occurred in a time-dependent manner. An ERK inhibitor (PD98059), a JNK inhibitor (SP600125), and proteasome/lysosome inhibitors all significantly reversed the reduction in Cx43 protein levels without any influence on the titer of progeny virus. In addition, CSFV activated ERK and JNK in a time-dependent manner and down-regulated Cx43 promoter activity, mainly through decreased AP2 binding. This effect was primarily caused by the replication of CSFV rather than a consequence of cytokines being induced by CSFV infection of endothelial cells.

H.-J. Hsiao and P. A. Liu contributed equally to this study.

H.-J. Hsiao · C.-Y. Wang (✉)
Department of Veterinary Medicine, National Chung Hsing University, 250 Kuo Kuang Road, Taichung 402, Taiwan
e-mail: cyoungwang@dragon.nchu.edu.tw

P.-A. Liu
Graduate Institute of Biotechnology, National Pingtung University of Science and Technology, Pingtung 912, Taiwan

H.-I. Yeh
Department of Internal Medicine, Mackay Memorial Hospital, Mackay Medical College, Taipei, Taiwan

Introduction

Classical swine fever virus (CSFV) is a small enveloped virus with a single-stranded (+) RNA genome of 12.5 kb belonging to the genus *Pestivirus* in the family *Flaviviridae*. The genome has a single open reading frame that encodes 12 structural and non-structural viral proteins [3, 4]. CSFV causes classical swine fever (CSF), which poses a significant threat to the pig industry, with high morbidity and mortality, and only a few countries have implemented vaccination programs. Due to its contagious nature and difficulty of control, it is a disease that is listed as notifiable to the OIE. The clinical symptoms of CSF are characterized by hemorrhagic diathesis, thrombosis, petechiation, leukopenia, and hematologic depletion in lymphoid organs; these symptoms can be mild or severe depending on age, breed, and virulence of the strain [3, 22]. Macrophages and endothelial cells are the primary sites for CSFV replication, and then lymphoreticular cells and certain epithelial cells become further predominant sites. CSFV up-regulates pro-inflammatory and pro-coagulant factors of endothelial cells and increases permeability, which triggers the sequential events associated with vascular dysfunction [3, 4]. This haemostatic imbalance and consumptive coagulopathy partly underlie the multiple hemorrhages of the organs caused by CSFV, but much remains unknown [4, 22]. Unlike other viral hemorrhagic diseases, such as African swine fever and dengue, the degradation of an initiator of the cascade of α/β interferon, interferon regulatory factor 3 (IRF3), is induced by the

CSFV protein, N^{pro}, and CSFV also blocks apoptosis of infected cells at various levels by inactivation of caspase-3, caspase-7, caspase-8, and the mitochondrial checkpoints, thereby establishing a long-term infection without causing a cytopathic effect [2, 4, 7, 13, 30].

Gap junctions made of connexin molecules mediate direct intercellular communication. In the endothelial monolayer of the vascular wall, these junctions contribute to the maintenance of the functional integrity of the cells [20, 33]. There is growing evidence to suggest that endothelial dysfunction is associated with several types of stress events, including high glucose, the presence of nicotine, and hyperlipidemia, and such dysfunction is associated with down-regulation of the gap junction [18, 28, 32, 34]. On the other hand, reduction of endothelial connexin 43 (Cx43) has been reported to enhance the expression of procoagulant factors directly [34]. Since CSFV has been shown to disturb the haemostatic balance, this raises the possibility that the endothelial gap junction is altered during infection. To this end, we examined the expression of Cx43, a member of connexin family that is predominantly expressed in endothelial cells, the integrity of the gap junctional intercellular communication (GJIC), and its signaling pathway following CSFV infection. Our data show that CSFV down-regulates the Cx43 and attenuates GJIC through the MAPK pathway. This effect can be attributed to the replication of CSFV and can be augmented by increasing the dose of CSFV used for infection.

Materials and methods

Virus, cells, and titration

The CSFV strain TW/05 (GenBank accession no. GQ396706), obtained from Dr. Ming-Tang Chou (National Pingtung University of Science and Technology, Taiwan), was propagated in the pig kidney cell line PK-15 with Dulbeccos modified Eagle's medium (DMEM) supplemented with 5% fetal calf serum. Virus purification was done following the procedures of Campos et al. [4] with the modification that only virus that was released into the supernatant was collected in order to ensure that cellular debris was eliminated. Virus titers were determined by an immunofluorescence method. At 48 hpi, PK-15 cells were dried and fixed with the neutral formalin (Fisher, USA) for 2 h. The cells were washed with phosphate-buffered saline (PBS) and incubated with pig anti-CSFV serum or a monoclonal antibody against the CSFV E2 glycoprotein (WH303; Veterinary Laboratories Agency, UK) for 1 h at 37°C. After washing, FITC-conjugated rabbit anti-pig IgG or Texas Red-conjugated anti-mouse Ig (Zymed, USA) was used as the secondary antibody. Finally, the cells were visualized by fluorescence microscopy, and virus titers were calculated and expressed as $TCID_{50}$/ml [25]. For the serial experiments, porcine aortic endothelial cells (PAECs) were obtained from Cell Applications Inc. (USA). These cells were isolated from healthy and plaque-free aorta and characterized previously [11]. They were grown in PAEC growth medium (Cat. No. P211-500), seeded at a density of 3×10^6 cells/ml, and infected with purified CSFV at a multiplicity of infection (M.O.I.) of 0.01–10 $TCID_{50}$ per cell as described previously [3]. UV-inactivated purified CSFV or culture medium alone was applied to cells as the mock control. For time course experiments, cells were infected with CSFV at an M.O.I. of 10 $TCID_{50}$ per cell for 0, 6, 12, 24, 36, and 48 h. For experiments testing dose dependence, cells were infected with CSFV at an M.O.I. of 0.01, 0.1, 1, and 10 $TCID_{50}$ per cell for 48 h. For drug experiments, PAECs were pre-treated with 25 μM leupeptin (Sigma, USA), a lysosomal inhibitor, plus 25 μM *N*-acetyl-leucyl-leucyl-norleucinal (ALLN) (Sigma, USA), a proteasomal inhibitor, 40 μM PD98059 (Sigma, USA), 15 μM SB203580 (Sigma, USA) or 10 μM SP600125 (Sigma, USA) for 60 min and then inoculated with an M.O.I. of 10 $TCID_{50}$ per cell of CSFV for 1.5 h at 37°C. For interleukin-1β (IL-1β) experiments, PAECs were inoculated with CSFV at an M.O.I. of 10 $TCID_{50}$ per cell, the inactivated supernatant from CSFV-infected cells, and 0.5 μg/ml of IL-1β (Calbiochem, USA). The inoculum was then removed and replaced with the growth medium with or without the same concentration of drugs. At 48 hpi, cells were lysed by freezing and thawing, and the progeny viruses of each group were titrated on PK-15 cells.

Western blotting

Cells were collected in a buffer containing 150 mM NaCl, 5 mM EDTA, 1% NP40, 2 mM PMSF and 50 mM Tris–HCl, pH 7.4, followed by sonication for 30 s. Thirty micrograms of sample was loaded into each lane, resolved by 12% SDS-PAGE, and transferred to a PVDF membrane (Amersham, UK). The membrane was incubated with anti-Cx43 antibody (Chemicon, USA), anti-non-phospho-Cx43 antibody (Zymed, USA), anti-JNK antibody (Cell Signaling Technology, USA), anti-phospho-JNK antibody (Upstate, USA), anti-p42/p44 Erk antibody (Cell Signaling Technology, USA), anti-phospho-p42/p44 Erk antibody (Cell Signaling Technology, USA) or anti-actin antibody (Chemicon, USA) at room temperature for 1 h. The cross-reactivity of antibodies with porcine proteins was confirmed previously. After washing with TBST (20 mM Tris, pH 7.6, 150 mM NaCl, and 0.1% Tween 20), a horseradish peroxidase-conjugated mouse anti-rabbit or donkey anti-mouse IgG (TBST plus 10% BSA), as appropriate, was added, and the membrane was then developed using an

enzyme-linked chemiluminescence system (ECL; Amersham, UK). For one group of drug experiments, the cells were treated with 25 μM leupeptin plus 25 ALLN, 40 μM of PD98059, 15 μM of SB203580 or 10 μM of SP600125. For both groups of drug experiments, the drugs were added 60 min prior to CSFV infection. Densitometric analysis was performed on immunoblots using Imagemaster (Amersham, USA), and the total amounts of Cx43 protein were divided by those of actin protein within each lane.

Immunofluorescence detection

At 48 hpi, cells on coverslips were fixed with methanol at −20°C for 5 min. After blocking with 0.5% BSA, the cells were incubated with anti-Cx43 antibody at 37°C for 1 h, followed by incubation with a CY3-conjugated donkey anti-mouse antibody (Chemicon, USA). The cells were then incubated with bisbenzamide (1 μg/ml; Sigma, USA) for 15 min, mounted, and examined using a Leica TCS SP confocal laser scanning microscope.

Semi-quantitative RT-PCR

Total RNA was extracted using Trizol Reagent (Invitrogen, USA) according to the manufacturer's instructions. The RNA was dissolved in RNase-free water and then treated with RNase-free DNase (QIAGEN, Germany) before quantification. Total RNA (2 μg) was reverse-transcribed into complementary DNA using SuperScript™ II reverse transcriptase and random primers and then diluted to a final volume of 20 μl. The optimal number of PCR cycle was determined for Cx43 (Cx-1: 5′-TCTGAGTGCCTGAACTTGC-3′ and Cx-2: 5′-ACTGACAGCCACACCTTCC-3′) and GADPH (GA-1: 5′-CATTGACCTCAACTACATGG-3′ and GA-2: 5′-TTGCCCACAGCCTTGGCAGC-3′) so that amplification was completed during an exponential phase. Cx43 primers were located separately in exon 1 and exon 2 of Cx43 gene (GenBank accession number: AK312324) with a 10,949-bp intron in between, which, under normal mRNA splicing, should result in a 188-bp fragment. Amplification of the GADPH transcript was used as an internal control. The amounts of Cx43 mRNA on the gel were divided by those of GADPH mRNA.

Reporter assay

The activity of the Cx43 promoter was determined using β-galactosidase and luciferase reporter assays (Promega, USA). The Cx43 promoter region spanning positions −164 to +23 was cloned into the luciferase vector and called −164-Cx43pGL3 [8]. Cells were first co-transfected with −164-Cx43pGL3 and CMVpβ-gal together and then infected with CSFV (10 M.O.I.). To identify the region of the Cx43 promoter that is affected by CSFV, cells were cotransfected with deletion mutants of −164-Cx43pGL3 (−83-Cx43pGL3, −46-Cx43pGL3, and −34-Cx43pGL3) and CMVpβ-gal and then infected with CSFV. At 48 hpi, the cells were lysed with 100 μl of 1× reporter lysis buffer, and 20 μl of lysate was used to measure both luciferase and β-galactosidase activities using a luminometer. The values of luciferase activity were normalized to an equal amount of β-galactosidase activity.

Nuclear protein preparation and electrophoretic mobility shift assay

Cells were infected with CSFV at an M.O.I. of 10 $TCID_{50}$, and nuclear extracts were isolated at the indicated time intervals. Briefly, 7×10^5 cells were washed with PBS, suspended in 200 μl of buffer A (10 mM HEPES, pH 8.0, 10 mM KCl, 1.5 mM $MgCl_2$, and 1 mM DTT), and incubated on ice for 10 min. After centrifugation at 20,000×*g* for 3 min, nuclear pellets were resuspended in 150 μl of buffer B (20 mM HEPES, pH 8.0, 1.5 mM $MgCl_2$, 420 mM NaCl, 0.2 mM EDTA, 1 mM DTT, and 25% glycerol) and kept on ice for 2 h. Samples were centrifuged at 14,000×*g* for 5 min, and the supernatant was stored at −70°C. Oligonucleotides used for electrophoretic mobility shift assay (EMSA) were as follows: NF-κB: 5′-CCACAGTTGGGATTTCCCAACCTGACCAG-3′ and AP2: 5′-CCCCCCAGCCCTT-3′. Nuclear extracts (5 μg) were incubated in 20 μl of reaction buffer containing 20 mM HEPES pH 8.0, 50 mM KCl, 0.5 mM DTT, 0.05 mM EDTA, 1 mM $MgCl_2$, 25% glycerol, 0.05% Igepal CA-630, and 0.2 μg of poly (dI-dC) for 20 min at room temperature. In competition experiments, a 100-fold molar excess of unlabeled oligonucleotides was added during the preincubation period to confirm the authenticity of these protein–DNA complexes. Results were obtained using a biotin-labeled EMSA kit (Panomics, USA) according to the manufacturer's instructions.

Scrape loading assay

At 48 hpi, GJIC in PAECs was evaluated by scrape loading assay. The medium from confluent cells was removed, and the cells were washed with Hank's balanced salt solution (Gibco, USA). A 27-gauge needle was used to create multiple scrapes through the cell monolayer in the presence of PBS containing 0.5% rhodamine-dextran and 0.5% lucifer yellow. After 3 min of incubation at room temperature, the culture was rinsed and then incubated for 10 min in PAEC growth medium to allow the loaded dye to transfer to adjoining cells. The cells were viewed and recorded using a fluorescence microscope. The area between the bilateral edges of lucifer yellow transfer and the scrape line was measured.

Analysis

All values are presented as mean (%) ±SE, and significant differences were analyzed by one-way ANOVA or *t* test.

Results and discussion

Down-regulation of both Cx43 protein and transcript by CSFV

At 48 hpi, no changes in cell density or cell morphology could be observed. The Cx43 proteins were abundantly expressed along the cell borders as typical plaques, and the size and number of plaques was gradually reduced in response to CSFV infection (Fig. 1). Western blotting verified the dose-dependent effect of CSFV on Cx43 expression. A significant reduction ($P < 0.05$) was observed at an M.O.I. of 1, and the relative amount of Cx43 protein was 76.3 ± 3.9% of the control cells. A more pronounced reduction was observed at an M.O.I. of 10, at which the Cx43 protein level was decreased to 62.7 ± 4.7% of that of the control cells (Fig. 2a). Similar to the total amount of Cx43 protein, CSFV exhibited a dose-dependent effect on the non-phosphorylated form of the Cx43 protein, a reduction of which was apparent at an M.O.I. of 0.1 (40.5 ± 3.7% reduction; $P < 0.05$) (Fig. 2b). The decrease in the Cx43 protein level was time-dependent, and significant reductions at an M.O.I. of 10 were seen at 24, 36, and 48 hpi, with relative levels of 86.4 ± 1.6, 67.7 ± 1.5, and 65.4 ± 3.2%, respectively, compared to the control cells (all $P < 0.05$, Fig. 2c). CSFV also had a dose-dependent down-regulating effect on Cx43 transcripts. At an M.O.I. of 1 and 10, their levels were decreased by 21.7 ± 1.4 and 32.0 ± 10.6%, respectively (both $P < 0.05$, Fig. 3a). At an M.O.I. of 10, a time-dependent down-regulation of Cx43 transcripts was evident, and significant reductions were seen at 36 and 48 hpi (32.1 ± 4.7 and 32.2 ± 2.2% decrease; both $P < 0.05$, Fig. 3b). This parallel decrease in Cx43 RNA and protein levels indicates that the decrease in the amount of Cx43 protein was due to a reduced level of Cx43 mRNA available for translation. In addition, a greater decrease in unphosphorylated Cx43 proteins than total Cx43 proteins suggested that the ratio of phospho-Cx43 protein to total Cx43 protein had increased. Consistent with this, an increase in the phosphorylation of Cx43 protein was accompanied by an impairment of GJIC [5]. Studies have shown that a wide range of cellular offenses, such as high glucose, the presence of nicotine, and treatment with angiotensin II and epidermal growth factor induces phosphorylation of the Cx43 protein through activation of protein kinase C, MAPK, and v-Src protein kinase [10, 14, 18, 19, 32]. Phosphorylation of tyrosine or serine residues is an initiator of degradation of the Cx43 protein by the proteasome and lysosome pathways [10, 14].

Down-regulation of the Cx43 promoter activity by CSFV through decreasing of AP2 binding activity

Reporter assays showed that all multiple transcription factors, except NF-κB, to a greater or lesser extent, contributed to the basal activity of the Cx43 promoter. Although AP1 is responsible for the maximal Cx43 promoter activity in cardiomyocytes, AP2 affects about 50% of the Cx43

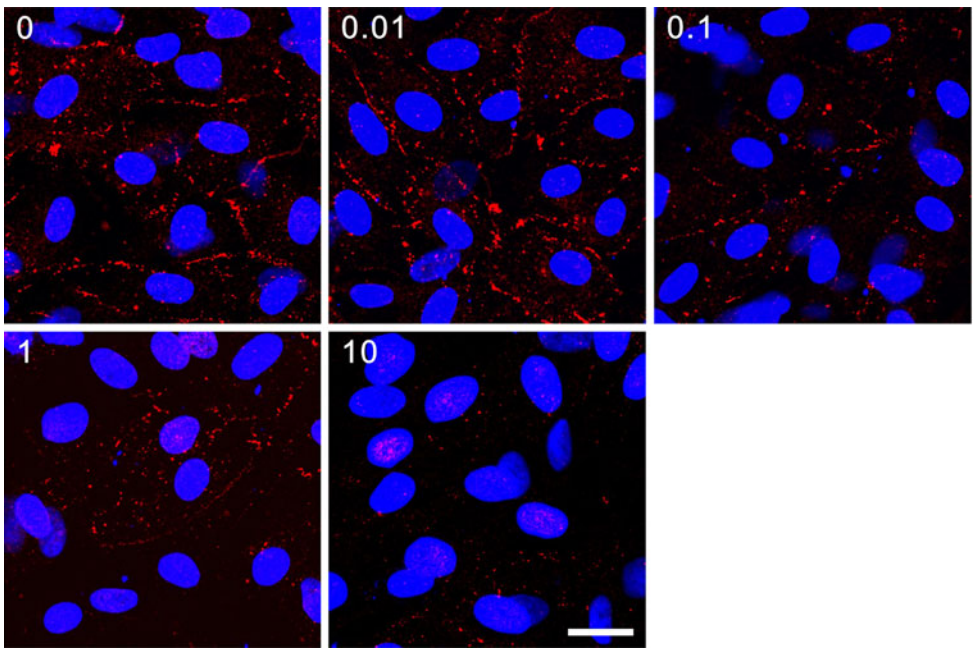

Fig. 1 Expression of Cx43 gap junctions in PAECs after CSFV infection, as evaluated by immunoconfocal microscopy. Compared to the control group, Cx43 gap junctions (*red spots*) are decreased in amount as the infectious dose of CSFV is increased. *Red label* Cx43, *blue label* nucleus. The M.O.I. in $TCID_{50}$ per cell is indicated in the *upper left* of each image. All images are at the same magnification. *Bar* 20 μm (colour figure online)

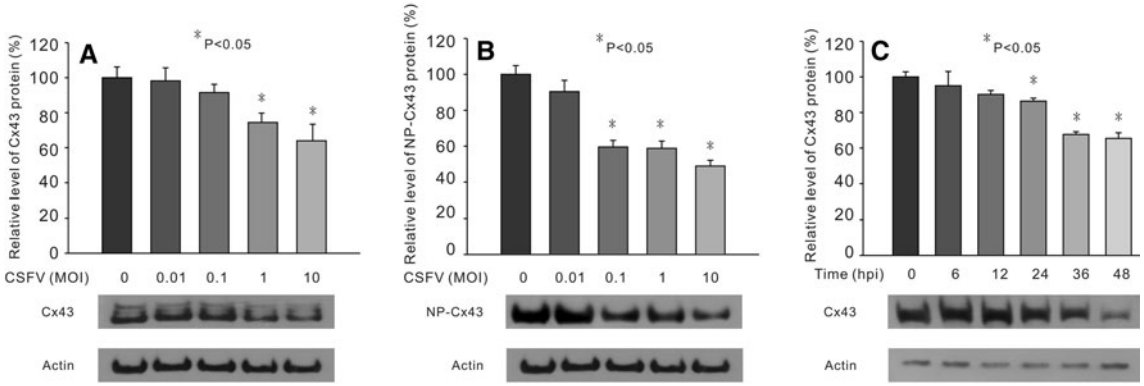

Fig. 2 Reduced expression of Cx43 (**a**) and non-phosphorylated Cx43 proteins (**b**) and time-dependence of reduction of expressed Cx43 proteins (**c**) in PAECs after CSFV infection, as detected by Western blotting. For each M.O.I. of CSFV or each hpi, the relative level of the total amount of Cx43 or non-phosphorylated Cx43 proteins, averaged from data of three independent experiments, is shown in a histogram at the *top* of the blot. $*P < 0.05$ compared to control cells

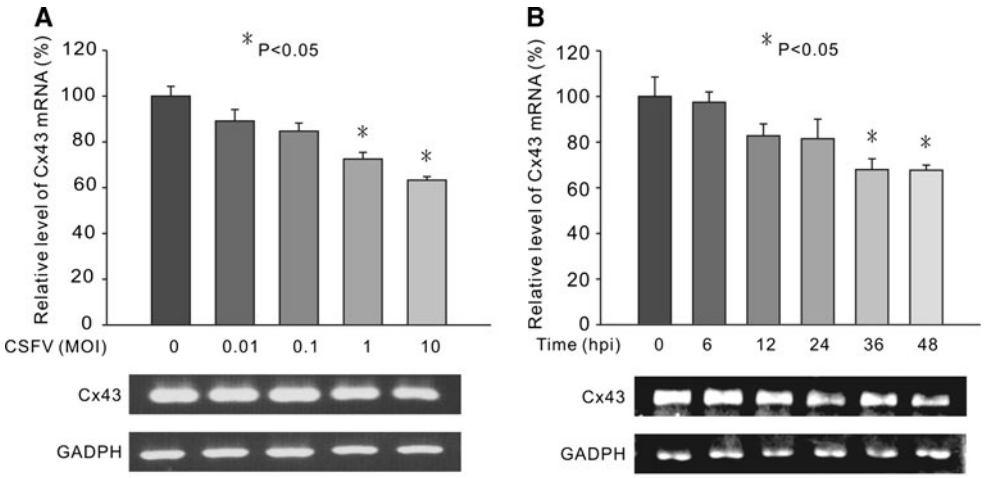

Fig. 3 Reduced transcription of Cx43 (**a**) and time-dependence of reduction of Cx43 transcripts (**b**) in PAECs after CSFV infection, as detected by semi-quantitative RT-PCR. For each M.O.I. or time point, the relative level of Cx43 transcripts is shown in a histogram at the *top* of the blot. $*P < 0.05$ compared to control cells

promoter activity in PAECs [27]. This discrepancy may result from the use of different cell types and promoter constructs. In addition, similar to the cooperative action between AP1 and SP1 for the Cx43 promoter activity reported in prostate cells, a synergy between AP2 and other factors may exist [12]. CSFV infection led to a dose-dependent reduction in Cx43 promoter-driven luciferase activity. At an M.O.I. of 1 and 10, compared to the control, the relative light units (RLUs) produced were reduced 44 ± 5.9 and $50 \pm 6.1\%$, respectively (both $P < 0.005$, Fig. 4a). This indicated that the Cx43 promoter activity was reduced at least twofold at an M.O.I. of 10. For the region of the Cx43 promoter affected by CSFV, a significant down-regulation was associated with positions -164 to -83, which includes two AP2-binding sites ($48 \pm 0.3\%$ reduction; $P < 0.005$). With the deletions between positions -83 to -64, no obvious differences were observed between control and infected cells. A slight increase in Cx43 promoter activity induced by CSFV was associated with positions -34 to $+148$, where a binding site for NF-κB is located (Fig. 4b). EMSA results further confirmed the above observations. The DNA-binding activities of AP2 decreased in a time-dependent manner but an increase in NF-κB binding was observed, with a maximal level at 12 hpi (Fig. 4c, d). Consistent with this, an association between NF-κB and attenuation of the gap junction has been found in myocytes and astrocytes treated with polyinosinic-cytidylic acid [36]. NF-κB is one of the downstream targets of MAPKs and is induced as a defensive response to injury, stress, and microbial pathogens [5, 15]. Promoter activities such as tissue factor and E-selectin have been proven to be up-regulated by NF-κB after CSFV infection [3, 24]. Taken together, our results show that down-regulation of Cx43 promoter activity by CSFV is dominated by the region of the promoter that stretches from positions -164 to -83 through decreased binding of AP2.

Attenuation of GJIC by CSFV

Attenuation of GJIC by CSFV was observed in the scrape loading assay. The green fluorescing lucifer yellow was

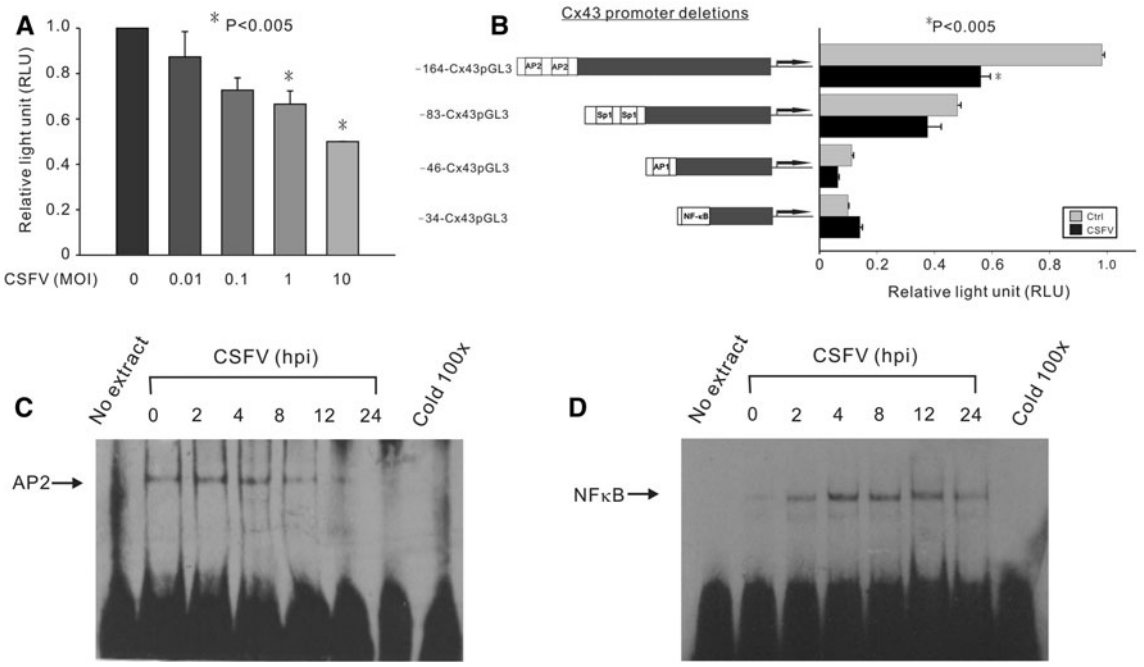

Fig. 4 Repression of Cx43 promoter activity by CSFV by decreasing AP2 binding activity. PAECs were co-transfected with −164-Cx43pGL3 and CMVpβ-gal and then infected with CSFV (**a**). Alternatively, PAECs were co-transfected with deletion mutants (−164-Cx43pGL3, −83-Cx43pGL3, −46-Cx43pGL3 or −34-Cx43pGL3) and CMVpβ-gal in the absence or presence of CSFV (**b**). At 48 hpi, luciferase activity was measured and normalized against β-galactosidase activity. Bars represent the mean ± SE of three independent experiments. *$P < 0.005$ compared to control cells (**a**) or the activity in the absence of CSFV (**b**); time course of the binding of transcription factors to their elements on the Cx43 promoter after CSFV infection, as measured by EMSA. PAECs were infected with CSFV for the indicated time intervals. Five micrograms of nuclear extract was prepared and incubated with biotin-labeled probes encoding AP2 (**c**) and NF-κB (**d**). *Arrows* denote the band location of the relevant transcription factor. For competition analysis, experiments were performed in the presence of excess unlabeled probes. A representative of three independent experiments is shown

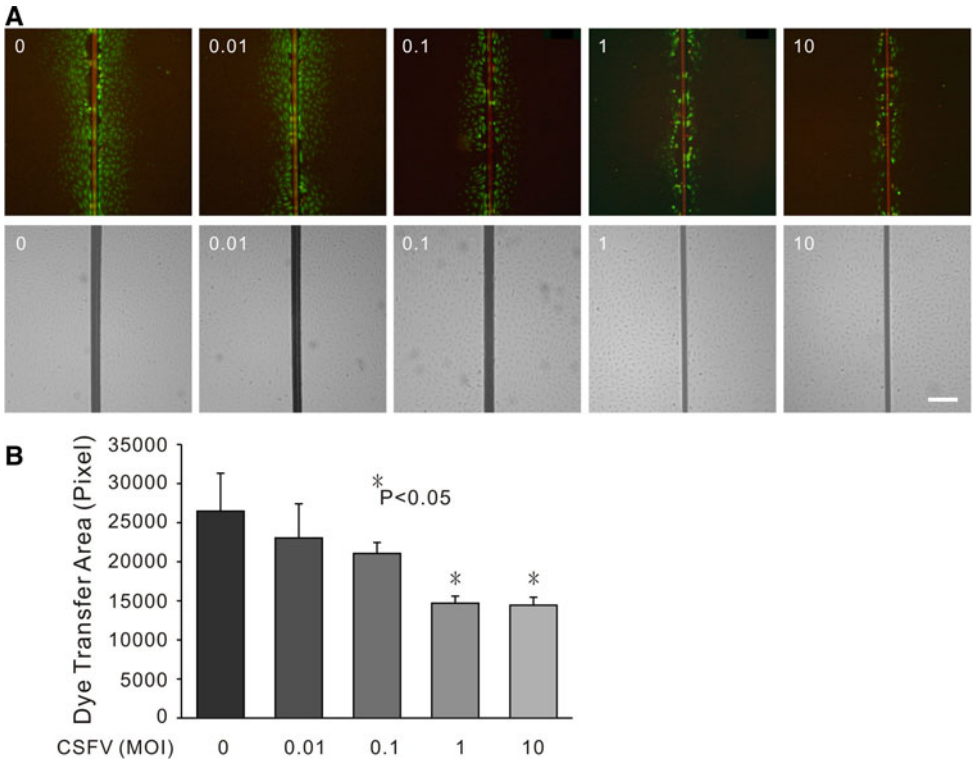

Fig. 5 Attenuation of gap junctional intercellular coupling by CSFV, as measured by scrape loading assay. The images at the *bottom* are phase-contrast micrographs of the upper fluorescent images (**a**). The M.O.I. is indicated in the *upper left* of each pair of images. All images are at the same magnification. *Bar* 20 μm. Analysis of the area between the bilateral edges of lucifer yellow transfer and the scrape line is shown in the histogram (**b**). *$P < 0.05$ compared to control cells

found to pass into adjacent cells in the controls; infection with CSFV decreased the area of spread (Fig. 5a). The relative area of dye transfer decreased in a dose-dependent manner, and infection at an M.O.I. of 1 and 10 resulted in 55.5 ± 3.4 and 54.5 ± 3.9% reductions, respectively (both $P < 0.05$, Fig. 5b). Similar findings have been seen in cells infected with certain RNA or tumor viruses [9]. Replication of feline immunodeficiency virus resulted in a 30% of decrease in the gap junction in both astroglia and kidney cells [6]. The release of tumor necrosis factor-α, IL-1β, interleukin-6, and interferon-γ upon borna disease virus (BVD) infection has been shown to inhibit astroglial Cx43 expression and functional coupling in rats [17, 23]. E5 protein of human papilloma virus was the first viral protein shown to impair the GJIC [1, 20]. It would be tempting to conclude that the down-regulation of Cx43 leading to an

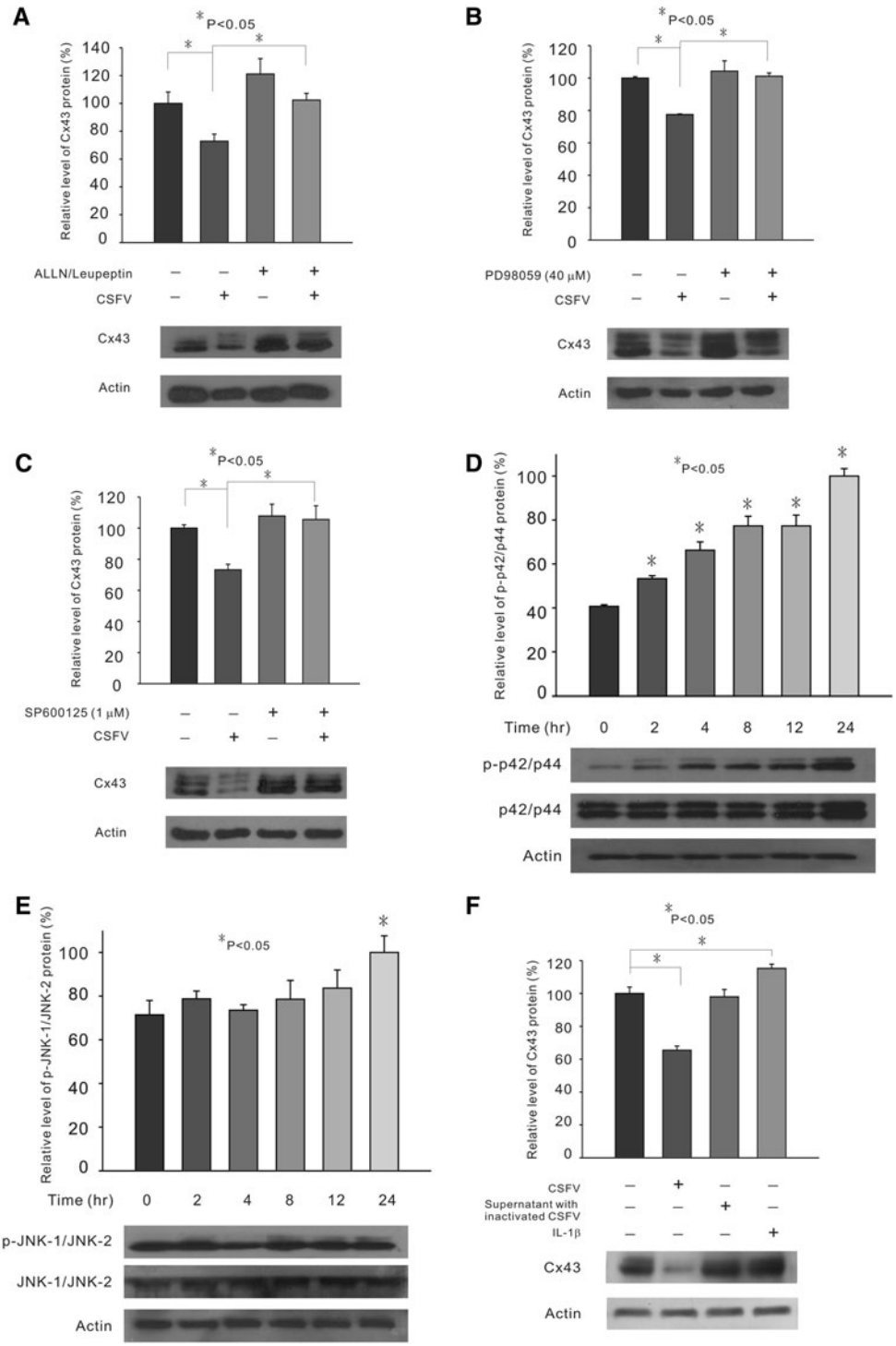

Fig. 6 Involvement of the lysosomal and proteasomal pathways, MAPK pathways, and cytokines in CSFV-induced Cx43 down-regulation. Reversal of the down-regulation of Cx43 protein by CSFV with leupeptin plus ALLN (**a**), PD98059 (**b**) or SB203580 (**c**), as detected by Western blotting; time-course of phosphorylation of ERK1/2 (**d**) and JNK1/2 (**e**) induced by CSFV, as detected by Western blotting; irrelevance of cytokines in the down-regulation of Cx43 induced by CSFV (**f**), as detected by Western blotting; The relative level of the total amount of Cx43 or the phosphorylated protein is shown in the histogram at the *top* of the blot. $*P < 0.05$ compared to control cells

Table 1 Titers of progeny virus from CSFV-infected cells in the presence or absence of inhibitors

CSFV inhibitor:	CSFV	CSFV ALLN/leupeptin	CSFV PD98059	CSFV SP600125	CSFV SB20358
Titers ($TCID_{50}$/ml)[a,b]:	$1.7 \pm 0.1 \times 10^6$	$2.1 \pm 0.5 \times 10^6$	$1.9 \pm 0.7 \times 10^6$	$1.1 \pm 0.2 \times 10^6$	$1.2 \pm 0.4 \times 10^6$

[a] The titers are mean plus standard error (mean ± SE) of four independent experiments

[b] All titers of progeny virus from CSFV-infected cells with inhibitors did not show significant differences versus the control group, $P > 0.05$

attenuated GJIC is likely to be a protective attempt used by infected cells or surrounding neighbors to prevent the intercellular transmission of death signals or spread of infection. In accordance with the above notion, when the GJIC of rat hepatocyte was blocked by a specific inhibitor, 1-(5-isoquinolinesulfonyl)-2-methylpiperazine at 40 μM, the plaques caused by herpes simplex virus completely disappeared [16].

Involvement of the lysosomal, proteasomal, and MAPK pathways in CSFV-induced Cx43 down-regulation

Cx43 protein turnover is involved in both the lysosomal and proteasomal pathways [19]. The co-administration of proteasome and lysosome inhibitors, leupeptin and ALLN, increased the basal level of Cx43 proteins, which reached 121.2 ± 11.1% of the control level. In addition, the down-regulation of Cx43 by CSFV was abrogated, and the relative amount of Cx43 protein was raised to the basal level (Fig. 6a). This might be caused by direct interference with the Cx43 transcriptional regulatory proteins or simply blockage of the degradation of Cx43 protein by inhibitors. Furthermore, potential signaling pathways involved in the down-regulation of Cx43 by CSFV were investigated. Both an ERK inhibitor (PD98059) and a JNK inhibitor (SP600125) reversed the reduction of Cx43 protein levels to 101.1 ± 2.1 and 105.5 ± 8.8% of the control ($P < 0.05$, Fig. 6b, c). In contrast, a p38 inhibitor (SB203580) did not affect CSFV-induced Cx43 down-regulation (data not shown). None of the MAPK inhibitors caused any noticeable alteration of the basal level of Cx43 protein or affected the titers of progeny virus (Table 1). In addition, ERK1/2 began to be significantly phosphorylated at 2 hpi and increased more than twofold at 24 hpi ($P < 0.05$, Fig. 6d). A more modest phosphorylation was seen with JNK, and a significant increase was only demonstrated at 24 hpi ($P < 0.05$, Fig. 6e). In accordance with our results, phosphorylation of ERK1/2 and JNK accompanied by down-regulation of Cx43 protein has been found in cardiomyocytes, epithelial cells, and endothelial cells treated with 12-*O*-teradecanoylphorbol-13-acetate and epidermal growth factor [14, 24, 26, 33]. Instead of phosphorylation of c-Jun, JNK activated by CSFV may ubiquitinate c-Jun, a component of AP1, to facilitate its degradation by the proteasome pathway, leading to the reduction of Cx43 promoter activity [8, 29]. The activation of JNK gradually increased at the late phase of infection, implying that a late product of viral replication or progeny virus is likely to participate in this process. Since either ERK or JNK inhibitors can reverse the down-regulation of Cx43 protein, there is a possibility that cross-talk between MAPKs is involved in the regulation of Cx43.

Irrelevance of cytokines in CSFV-induced Cx43 down-regulation

To clarify whether the down-regulation of Cx43 could be directly attributed to replicating CSFV or was a consequence of cytokines induced by CSFV in endothelial cells, the supernatant containing inactivated CSFV was inoculated into PAECs. The Cx43 protein remained unchanged, and the relative level was 97.9 ± 4.4% of the control level (Fig. 6f). This indicated that pro-inflammatory cytokines induced by CSFV, such as interleukin-1α and interleukin-6, did not affect the expression of Cx43 [4]. In addition, there was also a possibility that the level of secreted cytokines was insufficient to affect the expression of Cx43. Studies have shown that IL-1β mRNA and arginase-1 in macrophages increase significantly after CSFV infection and subsequently counteract each other [35]. Our data obtained with endothelial cells are consistent with those of other studies suggesting that the Cx43 protein is up-regulated by exogenous IL-1β, and the relative level was 115.3 ± 2.6%

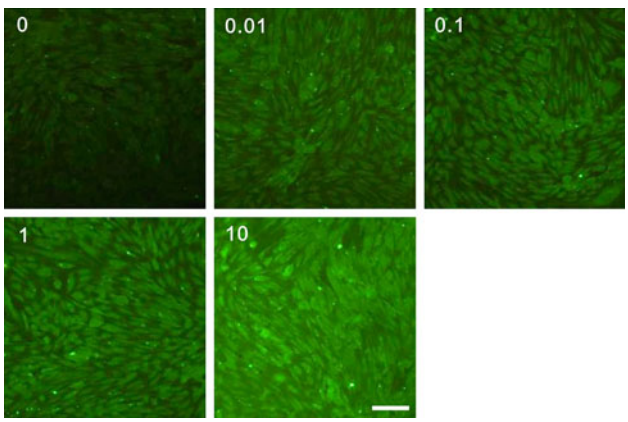

Fig. 7 Dose-dependent increase in immunofluorescence intensity in PAECs after CSFV infection. The M.O.I. of $TCID_{50}$ per cell is indicated in the *upper left* of each image. All images are at the same magnification. *Bar* 200 μm

Table 2 Titers of progeny virus from cells infected with different doses of CSFV

Infection dose of CSFV (M.O.I. in $TCID_{50}$/cell)	0.01	0.1	1	10
Titers of progeny virus ($TCID_{50}$/ml)[a]	$1 \pm 5.2 \times 10^1$	$8.3 \pm 5.9 \times 10^2$	$1.4 \pm 2.2 \times 10^5$	$2.3 \pm 1.4 \times 10^6$

[a] The titers are mean plus standard errors (mean ± SE) of three independent experiments

of the control level ($P < 0.05$ compared to the control group, Fig. 6f) [21, 31].

A direct relationship between the yield of progeny virus and the infectious dose of CSFV

The immunofluorescence signals represented the amount of E2 glycoproteins inside the infected cells originating from the progeny virus. No signals were observed in the mock control. In accordance with recent studies demonstrating that 97% of PAECs inoculated at an M.O.I. of 0.01 of $TCID_{50}$ per cell were infected at 48 hpi [4], nearly all cells infected at an M.O.I. of 0.01 showed green fluorescence despite a few variations, and this could be observed in repeated experiments. It is worth noting that the increase in immunofluorescence intensity was direct proportional to the inoculum dose (Fig. 7). Moreover, the titers of progeny viruses from cells infected with CSFV and the inoculated doses were in direct proportion (Table 2). This indicates that the yield of progeny virus depends primarily on how much virus was used for inoculation and on replication in the cells, which subsequently affected the degree of down-regulation of GJIC.

Down-regulation of PAEC Cx43 by CSFV may contribute to the pathogenesis of CSF in animals. Our recent study using an siRNA specific for Cx43 to decrease the expression of Cx43 in cultured human endothelial cells showed that reduction of Cx43 per se activated endothelial cells to pathological status, as characterized by up-regulation of plasminogen activator inhibitor I and von Willebrand factor, and impairment of proliferation, viability, and angiogenesis of the cells [33]. Since plasminogen activator inhibitor I and von Willebrand factor enhance coagulation, this finding is consistent with previous reports that CSFV disturbed the haemostatic balance [4]. In addition, the impairment of normal endothelial physiology due to reduction of Cx43 may delay the recovery of endothelium from CSFV infection.

In summary, this study, for the first time, shows that CSFV, in addition to inducing blockage of cellular antiviral and apoptotic responses, down-regulates Cx43 and attenuates the GJIC [3, 15]. Further investigation is warranted in order to identify the cellular protein(s) or CSFV component(s) that participate in this event. Our findings could provide further understanding of how CSFV promotes its pathogenesis by persisting inside cells to maintain production of progeny virus through a modulation of cellular physiology.

Acknowledgments This work is supported by the grant NSC-95-2313-B-020-005 awarded to Dr. C. Y. Wang from the National Science Council, Taiwan. Dr. Hung-I Yeh thanks the Mackay Memorial Hospital, Taiwan (MMH-E 97003), for support.

References

1. Aasen T, Hodgins MB, Edward M, Graham SV (2003) The relationship between connexins, gap junctions, tissue architecture and tumor invasion, as studied in a novel in vitro model of HPV-16-associated cervical cancer progression. Oncogene 22:7969–7980
2. Bauhofer O, Summerfield A, Sakoda Y, Tratschin J, Hofmann MA, Ruggli N (2007) Classical swine fever virus N^{pro} interacts with interferon regulatory factor 3 and induces its proteasomal degradation. J Virol 81:3087–3096
3. Bensaude E, Turner JLE, Wakeley PR, Sweetman DA, Pardieu C, Drew TW, Wileman T, Powell PP (2004) Classical swine fever virus induces proinflammatory cytokines and tissue factor expression and inhibits apoptosis and interferon synthesis during the establishment of long-term infection of porcine vascular endothelial cells. J Gen Virol 85:1029–1037
4. Campos E, Revilla C, Chamorro S, Alvarez B, Ezquerra A, Dominguez J, Alonso F (2004) In vitro effect of classical swine fever virus on a porcine aortic endothelial cell line. Vet Res 35:625–633
5. Crow DS, Beyer EC, Paul DL, Kobe SS, Lau AF (1990) Phosphorylation of connexin43 gap junction protein in uninfected and Rous sarcoma virus-transformed mammalian fibroblasts. Mol Cell Biol 10:1754–1763
6. Danave IR, Tiffany-Castiglioni E, Zenger E, Barhoumi R, Burghardt RC, Collisson EW (1994) Feline immunodeficiency virus decreases cell-cell communication and mitochondrial membrane potential. J Virol 68:6745–6750
7. Doceul V, Charleston B, Crooke H, Reid E, Powell PP, Seago J (2008) The Npro product of classical swine fever virus interacts with IkappaBalpha, the NF-kappaB inhibitor. J Gen Virol 89:1881–1889
8. Echetebu CO, Ali M, Izban MG, MacKay L, Garfield RE (1999) Localization of regulatory protein binding sites in the proximal region of human myometrial connexin43 gene. Mol Hum Reprod 5:757–766
9. Faccini AM, Cairney M, Ashrafi GH, Finbow ME, Campo MS, Pitts JD (1996) The bovine papilloma virus type 4 E8 protein binds to ductin and causes loss of gap junctional intercellular communication in primary fibroblast. J Virol 70:9041–9045
10. Girao H, Pereira P (2003) Phosphorylation of connexin43 acts as a stimuli for proteasome-dependent degradation of the protein in lens epithelial cells. Mol Vis 9:24–30
11. Hayama E, Imamura S, Wu C, Nakazawa M, Matsuoka R, Nakanishi T (2006) Analysis of voltage-gated potassium channel beta1 subunits in the porcine neonatal ductus arteriosus. Pediatr Res 59:167–174

12. Hernandez M, Shao Q, Yang XJ, Luh SP, Kandouz M, Batist G, Laird DW, Alaoui-Jamali MA (2006) A histone deacetylation-dependent mechanism for transcriptional repression of the gap junction gene Cx43 in prostate cancer cells. Prostate 66:1151–1161
13. Johns HL, Bensaude E, La Rocca SA, Seago J, Charleston B, Steinbach F, Drew T, Crooke H, Everett H (2010) Classical swine fever virus infection protects aortic endothelial cells from pIpC-mediated apoptosis. J Gen Virol 91(Pt 4):1038–1046
14. Kanemitsu MY, Lau AF (1993) Epidermal growth factor stimulates the disruption of gap junctional communication and connexin43 phosphorylation independent of 12-*O*-tetradecanoylphorbol 13-acetate-sensitive protein kinase C: the possible involvement of mitogen-activated protein kinase. Mol Biol Cell 4:837–848
15. Karin M, Lin A (2002) NF-kappaB at the crossroads of life and death. Nat Immunol 3:221–227
16. Knabb MT, Danielsen CA, Mchane-Kay K, Mbuy GKN, Woodruff R (2007) Herpes simplex virus-type 2 infectivity and agents that block gap junctional intercellular communication. Virus Res 124:212–219
17. Koster-Patzlaff C, Hosseini SM, Reuss B (2007) Persistent borna disease virus infection changes expression and function of astroglial gap junctions in vivo and in vitro. Brain Res 1184:316–332
18. Kuroki T, Inoguchi T, Umeda F, Ueda F, Nawata F (1998) High glucose induces alteration of gap junction permeability and phosphorylation of connexin43 in cultured aortic smooth muscle cells. Diabetes 47:931–936
19. Liang JG, Tadors PN, Westphale EM, Beyer EC (1997) Degradation of connexin43 gap junctions involves both the proteasome and the lysosome. Exp Cell Res 236:482–492
20. Lo CW (1996) The role of gap junction membrane channels in development. J Bioenerg Biomembr 28:379–385
21. Meme W, Ezan P, Venance L, Glowinski J, Giaume C (2004) ATP-induced inhibition of gap junctional communication is enhanced by interleukin-1 beta treatment in cultured astrocytes. Neuroscience 126:95–104
22. Moennig V, Floegel-Niesmann G, Greiser-Wilke I (2003) Clinical signs and epidemiology of classical swine fever: a review of new knowledge. Vet J 165:11–20
23. Ovanesov MV, Sauder C, Rubin SA, Richt J, Nath A, Carbone KM, Pletnikov MV (2006) Activation of microglia by borna disease virus infection: in vitro study. J Virol 80:12141–12148
24. Petrich BG, Gong X, Lerner DL, Wang X, Brown JH, Saffitz JE, Wang Y (2002) c-Jun N-terminal kinase activation mediates downregulation of connexin43 in cardiomyocytes. Circ Res 91:640–647
25. Reed IJ, Muench RH (1938) A simple method to estimating fifty percent end points. Am J Hyg 27:493–497
26. Rivedal E, Leithe E (2005) Connexin43 synthesis, phosphorylation, and degradation in regulation of transient inhibition of gap junction intercellular communication by the phorbol ester TPA in rat liver epithelial cells. Exp Cell Res 302:143–152
27. Salameh A, Krautblatter S, Baessler S, Karl S, Rojas Gomez D, Dhein S, Pfeiffer D (2008) Signal transduction and transcriptional control of cardiac connexin43 up-regulation after alpha1-adrenoceptor stimulation. J Pharmacol Exp Ther 326:315–322
28. Sato T, Haimovici R, Kao R, Li AF, Roy S (2002) Down-regulation of connexins expression by high glucose reduces gap junction activity in microvascular endothelial cells. Diabetes 51:1565–1571
29. Shyu KG, Wang BW, Yang YH, Tsai SC, Lin S, Lee CC (2004) Amphetamine activates connexin43 gene expression in cultured neonatal rat cardiomyocytes through JNK and AP-1 pathway. Cardiovasc Res 63:98–108
30. Summerfield A, Alves M, Ruggli N, de Bruin MG, McCullough KC (2008) High IFN-alpha responses associated with depletion of lymphocytes and natural IFN-producing cells during classical swine fever. J Interferon Cytokine Res 20:448–456
31. Tonon R, D'Andrea P (2002) The functional expression of connexin43 in articular chondrocytes is increased by interleukin 1beta: evidence for a Ca^{2+}-dependent mechanism. Biotechnology 39:153–160
32. Tsai CH, Yeh HI, Tian TY, Lee YN, Ko YS (2004) Down-regulating effect of nicotine on connexin43 gap junctions in human umbilical vein endothelial cells is attenuated by statins. Eur J Cell Biol 82:589–595
33. Wang HH, Kung CI, Tseng YY, Lin YC, Chen CH, Tsai CH, Yeh HI (2008) Activation of endothelial cells to pathological status by down-regulation of connexin43. Cardiovasc Res 79:509–518
34. Yeh HI, Lu CS, Wu YJ, Chen CC, Hong RC, Ko YS, Shiao MS, Severs NJ, Tsai CH (2003) Reduced expression of endothelial connexin37 and connexin40 in hyperlipidemic mice: recovery of connexin37 after 7-day simvastatin treatment. Atheroscler Thromb Vas Biol 20:1753–1762
35. Zaffuto KM, Piccone ME, Burrage TG, Balinsky CA, Risatti GR, Borca MV, Holinka LG, Rock DL, Afonso CL (2007) Classical swine fever virus inhibits nitric oxide production in infected macrophages. J Gen Virol 88:3007–3012
36. Zhao Y, Rivieccio MA, Lutz S, Scemes E, Brosnan CF (2006) The TLR3 ligand polyI:C downregulates connexin43 expression and function in astrocytes by a mechanism involving the NF-kappaB and PI3 kinase pathways. Glia 54:775–785